Research Article

Vivek D. Kalyankar*, and Gautam P. Chudasama

Influence of electrode tip diameter on metallurgical and mechanical aspects of spot welded duplex stainless steel

https://doi.org/10.1515/htmp-2020-0055
received September 20, 2018; accepted December 28, 2018

Abstract: In this article, the influence of electrode tip diameter is investigated for spot welded duplex stainless steel (DSS). Electrode tip diameter and welding current are considered as the major influencing parameters and their values are varied within the feasible range, suitable for 0.8 mm thick sheet, whereas other important parameters such as welding time and electrode force are kept constant. DSS with the chosen thickness range is now becoming a useful material in automotive body-in-white applications and in future it will become one of the key materials replacing the existing materials and hence research outcome of the present work may be beneficial from application view point. In this work, the spot welding quality is inspected through metallurgical aspects (microstructure and microhardness), physical aspects (nugget diameter and electrode indentation), mechanical performance (tensile shear strength [TSS]) and failure mode. The obtained result shows that smaller electrode tip diameter limits nugget diameter due to expulsion phenomena and increases electrode indentation due to higher current intensity. TSS decreases with increase in electrode tip diameter for the same welding current but maximum TSS obtained for particular electrode tip diameter increases with increase in electrode tip diameter up to a specific limit and then it remains constant.

Keywords: resistance spot welding, duplex stainless steel, electrode tip diameter, welding current, tensile shear strength, nugget diameter

*** Corresponding author: Vivek D. Kalyankar,** Mechanical Engineering Department, S V National Institute of Technology, Surat, Gujarat, India, e-mail: vivekkalyankar@yahoo.co.in, tel: +91-951-082-8842
Gautam P. Chudasama: Mechanical Engineering Department, Indus Institute of Technology & Engineering, Ahmedabad, Gujarat, India, e-mail: gautamchudasama16@gmail.com
ORCID: Vivek D. Kalyankar 0000-0002-7141-3705;
Gautam P. Chudasama 0000-0002-9593-664X

1 Introduction

Nowadays, automobile industries are making efforts to build safer, lighter and more fuel efficient vehicles. To achieve this goal, materials such as advanced grade of steels, fibres and aluminium alloys are getting used in body-in-white applications [1]. Out of these materials, stainless steel has good potential to improve vehicle performance by reducing vehicle weight because of its excellent strength and formability [2]. Furthermore, next-generation vehicle programme confirmed the possibility of stainless steel as a structural material in automobile sector [3]. This programme revealed that stainless steel not only reduces vehicle weight but also at the same time increases safety, sustainability and environmental resistance of structural automotive systems [2]. Stainless steel can be applicable in subframes, bumper beam, A and B-pillars, door pillar, crash boxes, rollover bars, seat rails, fuel rail assemblies and suspension/wheel housings [2,4,5].

Resistance spot welding (RSW) is a dominant process for joining sheet metal components in automobile industries [6]. Typically, there are 3,000–5,000 spot welded joints in a body-in-white of modern vehicles [7]. RSW is a conventional process, even it is also used in various industries because of its simplicity, narrow heat affected zone (HAZ), energy efficiency and ease of automation [8]. In automotive structural assemblies, load is transferred through groups of spot welds during crash. Furthermore, spot welds can act as fold initiation sites to manage impact energy. Moreover, failure of spot welding is identified as a key failure during the vehicle crash. Hence, strength, stiffness and integrity of car body are greatly affected by the quality of spot welds [7]. Therefore, detailed metallurgical and mechanical study of stainless steel spot welded joint is necessary before use in automotive structural parts.

In the past, detailed study about spot welding of austenitic stainless steel [9–11], ferritic stainless steel [2,12,13] and martensitic stainless steel [14–16] has been

carried out. However, very limited literature is available about the investigation of duplex stainless steel (DSS). It is identified that DSS is an excellent candidate material for automobile structural applications due to the combination of higher mechanical properties and corrosion resistance [17,18]. It is more suitable for crumple zones to absorb the energy during crash due to strain hardening and favourable behaviour at a higher strain rate [19,20]. Also, DSS does not have martensitic transformation and related problem during spot welding. Therefore, the use of DSS is a good solution to avoid welding problems of martensite-containing advanced high strength steel [2,5]. Pouranvari et al. [2] and Alizadeh-Sh et al. [21] concluded that the fast cooling rate of RSW and the presence of TiC particles hindered the post solidification transformation of ferrite to austenite and results in unbalanced phases in the microstructure. Arabi et al. [5] investigated the effect of welding current on microstructure and mechanical behaviour for RSW of 2304 DSS. Arabi et al. [22] suggested downsloping technique and *in situ* post weld annealing to improve phase balance for DSS, but all the joints failed in the interfacial failure (IF) mode. Keeping in view various advantages of DSS and its possible applicability in automobile sector, it is very essential to have in-depth research on various joining aspects of DSS. Furthermore, mechanical behaviour of spot welded DSS is controlled by ferrite/austenite phase balance and absence of precipitates such as Cr_2N, sigma and chi. However, these factors are affected by the fast cooling rate of resistance spot welded joint.

Literature demonstrates that mechanical behaviour of spot welded joint is mostly affected by welding current, followed by welding time and electrode force [23]. Furthermore, some process parameters and material conditions such as holding time [24], surface characteristics [25], preheating [26], post heating [27], alloy content [28] and multi pulse [29] are also investigated. However, there is further scope to improve the mechanical performance of spot welded joint by electrode tip diameter. Mikno and Bartnik [30] studied the effect of electrode diameter and bevel angle on heating of electrodes and tensile shear strength (TSS) for low carbon steel. Bayramoglu et al. [31] studied the effect of electrode tip radius, sheet thickness and welding parameters on TSS and nugget diameter for low carbon steel.

Keeping in view the suitability and applicability of DSS in automotive sector as well as a possible scope to enhance its performance with critical control on electrode tip diameter, attempt is made in this article to present an in-depth study of the influence of electrode tip diameter on mechanical behaviour of spot welded 2205 DSS. Moreover, this study also examined the effect of electrode tip diameter and welding current on microstructure, microhardness, nugget diameter, electrode indentation, TSS and failure mode. Section 2 describes the experimental procedure executed to carry out necessary experimental work.

2 Experimental procedure

A 0.8 mm 2205 DSS is used as a base metal (BM), and its chemical composition is presented in Table 1. The as-received material possesses a yield strength of 655 MPa and an ultimate tensile strength of 777.6 MPa. Spot welding is carried out using a three-phase AC inverter spot welding machine (i4; Prospot). Cu–Cr–Zr electrodes with variable tip diameter and having 45° truncated cone are used to obtain necessary spot joints. Squeeze time, weld time, hold time and electrode pressure are kept constant at 1,999 ms, 240 ms, 1,000 ms and 4.5 bar, respectively. Based on the trial experiments, electrode tip diameter is selected from 5 to 7 mm in increment of 1 mm and welding current from 4 to 7.5 kA in step of 0.5 kA. Three samples are prepared for each run and out of these, two are used for the tensile shear test and one for metallurgical examination. Spot welded joint has more tendency to fail in the IF mode for the tensile shear test compared to other tests such as peel test and cross tension test [6,32]. Furthermore, it is observed that if spot weld joint fails in the pull-out failure (PF) mode during the tensile shear test, then it will also show failure behaviour with the PF mode during the peel test as well as the cross tension test [7]; therefore, the tensile shear test is carried out to investigate the mechanical performance of spot welded joint. Table 2 shows the

Table 1: Chemical composition of DSS under consideration

BM	C	Cr	Ni	Mo	Mn	Si	N	P	S
2205	0.018%	22.27%	5.45%	3.02%	1.27%	0.39%	0.20%	0.025%	0.003%

Table 2: Parameter setting and measured responses for various experiments

Expt. no.	Electrode tip diameter (mm)	Weld current (kA)	Peak load (kN)	Nugget diameter (mm)
1	5	4	6.85	3.572
2	5	4.5	10.77	3.951
3	5	5	11.58	4.229
4	5	5.5	12.07	4.504
5	5	6	13.43	4.8
6	5	6.5	12.42	4.739
7	5	7	12.61	3.862
8	6	4	10.67	3.0
9	6	4.5	10.7	3.848
10	6	5	10.19	3.4
11	6	5.5	12.3	4.745
12	6	6	13.16	4.45
13	6	6.5	13.26	5.2
14	6	7	13.93	5.6
15	6	7.5	13.20	5.382
16	7	4	9.74	2.864
17	7	4.5	9.97	2.744
18	7	5	11.05	3.497
19	7	5.5	10.85	3.874
20	7	6	11.66	4.1
21	7	6.5	13.14	4.644
22	7	7	12.19	5.544
23	7	7.5	13.39	6.318

parameter setting considered during each experiment as well as measured responses, which are based on the average values of two individual experimental runs.

Figure 1 shows the standard tensile shear specimen as per AWS D8.9:2012 standard [33], and the same is considered in the present work. The tensile shear test is carried out using universal testing machine (UTES-40; EIE Pvt Ltd) at the speed of 10 mm/min [33]. To study the metallurgical properties of the spot welded sample, it is cut slightly offset from its weld centreline and metallurgical samples are prepared according to the standard metallurgical procedures. To reveal the macrostructure, Marble etchant (50 mL HCl, 50 mL H_2O and 10 g $CuSO_4$) is used, whereas for microstructure, Kalling's No. 1 etchant (1.5 g $CuCl_2$, 33 mL HCl, 33 mL H_2O and 33 mL C_2H_5OH) is used [2,5]. Nugget diameter is measured with the help of a vision measuring system (SDM-TRZS 300; Sipcon, India). Microexamination is carried out on an inverted optical microscope (Observer A1M; Carl Zeiss). Microhardness testing is carried out in the diagonal transverse direction from the BM of top coupon to the BM of bottom coupon using the Vickers microhardness tester (HM-211; Mitutoyo) at constant loads of 200 g and 1 kg [33].

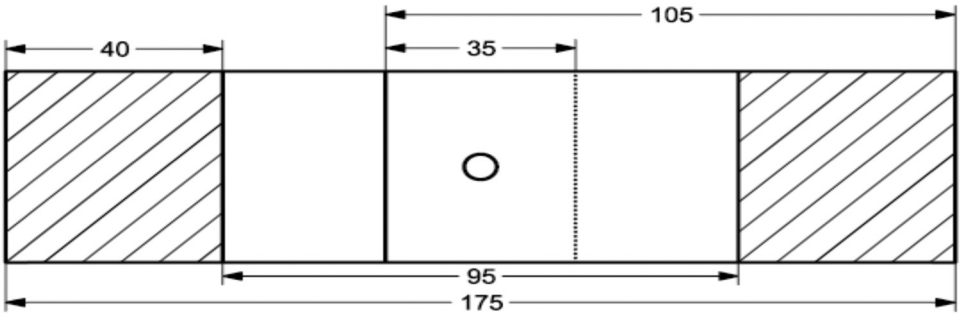

Figure 1: Tensile shear specimen as per AWS D8.9:2012 standard.

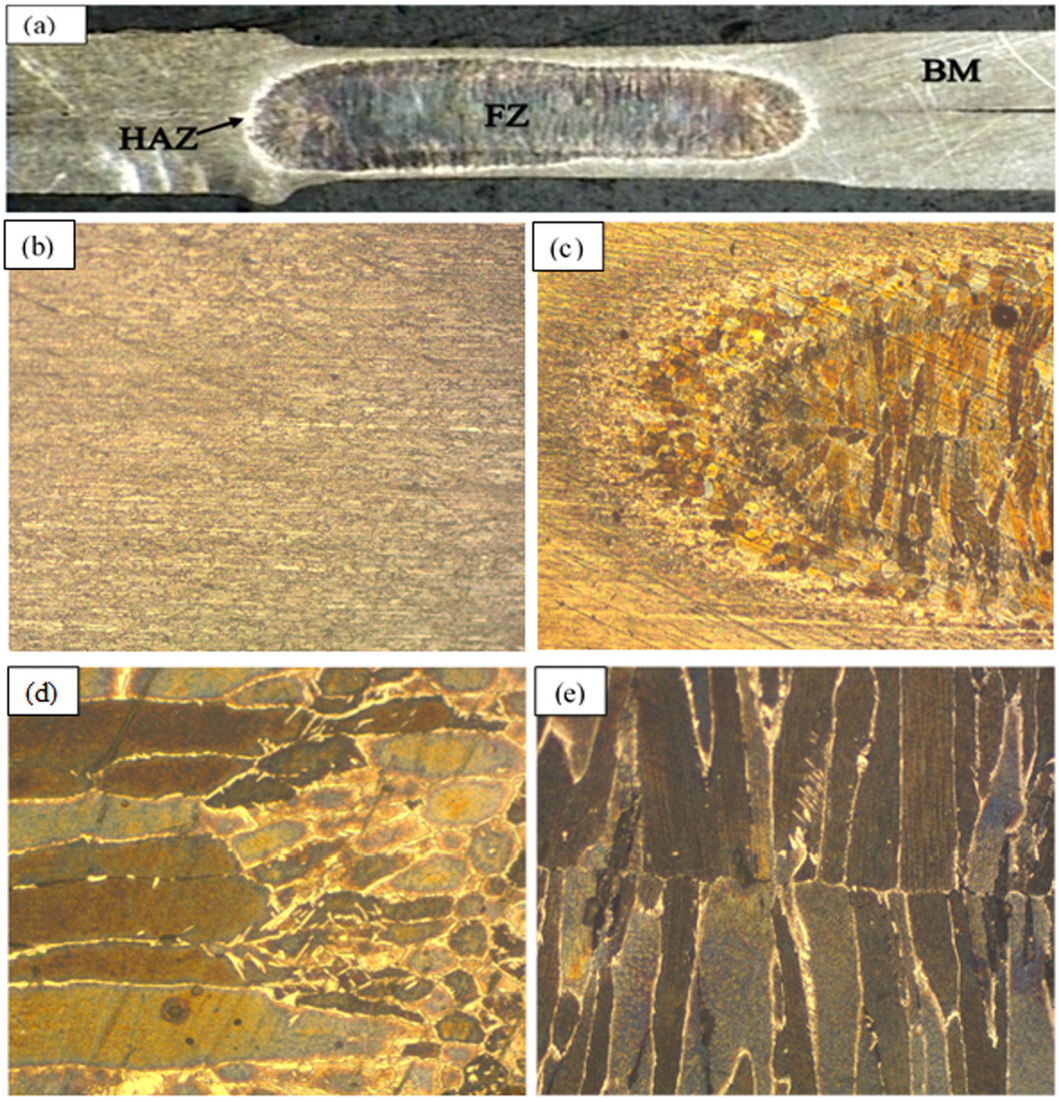

Figure 2: Macro/microstructure of 2205 DSS spot welded joint: (a) macrostructure, (b) BM microstructure, (c) BM/HAZ/FZ interface, (d) equiaxed grain/columnar grain interface and (e) columnar grain structure at FZ centre (lighter phase is austenite and darker one is ferrite).

3 Results and discussion

Welding quality of spot welded joint is assessed though metallurgical aspects (microstructure and microhardness), physical aspects (nugget diameter and electrode indentation), mechanical aspect (TSS as a peak load) and failure mode. Efforts are made in this work to consider all these aspects, and the results obtained for all the individuals are discussed in the following subsections.

3.1 Metallurgical aspects

Figure 2(a) shows the macrostructure of welded joint (electrode tip diameter: 6 mm and welding current: 6 kA), indicating good weld with distinct fusion boundary and narrow HAZ. Figure 2(b) shows the microstructure of BM which consists of 50% ferrite and 50% austenite. Figure 2(c) shows that fusion zone (FZ) microstructure has the columnar grain structure at centre and the equiaxed grain structure in the narrow region near the fusion boundary. This is due to the formation of chilled zone at the fusion boundary, where the cooling rate is higher which results in faster nucleation of small equiaxed grains in the random direction at the nugget edge and forms the equiaxed grains region similar to the chilled zone in the casting process. The columnar grains at the centre of nugget are observed due to possible evolution and growth of equiaxed grains along possible easiest directions, which

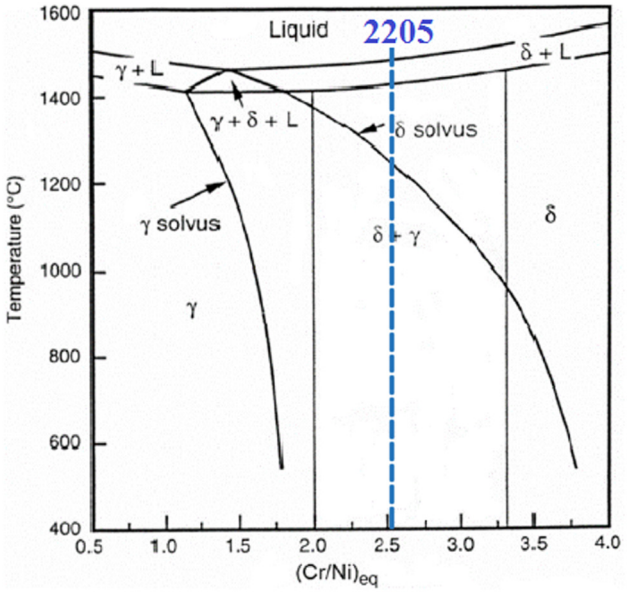

Figure 3: Pseudo binary diagram of stainless steel [34].

is generally opposite to the direction of heat flow, towards the centre of the nugget. Figure 2(d) and (e) shows the microstructure of edge of FZ and centre of FZ, respectively, which consist of ferrite (dark portion) and austenite (light portion), indicating less percentage of austenite compared to ferrite. According to chemical composition of 2205 DSS, the chromium to nickel equivalent ratio is 2.51 and solidification and post solidification path for 2205 DSS is summarised as follows from welding research counselling (WRC) – 1998 diagram which is shown in Figure 3 [34].

$$L \rightarrow L + F \rightarrow F \rightarrow F + A \rightarrow F + A + \text{Precipitation},$$

where L = liquid, F = ferrite and A = austenite.

From the WRC diagram, during solidification, 100% ferrite is formed and it is stable at elevated temperature. When temperature falls below the ferrite solvus temperature, post solidification transformation of ferrite to austenite occurred by nucleation and growth process and results in complete coverage of ferrite grain boundaries by austenite. Additional austenite is also formed intragranularly within the ferrite grains, but the fast cooling rate of RSW hindered the post solidification transformation of ferrite to austenite, which results in unbalanced microstructure of FZ.

Figure 4 shows the microstructure for different weld currents with 6 mm electrode tip diameter, indicating that volume fraction of austenite is more and covers entire grain boundaries for 7 kA compared to a lower current of 4 kA. Additionally, intergranular austenite is also observed for high welding current. This is attributed to the fact that with increase in welding current, heat generation in FZ increases, i.e. temperature of FZ that increases total available time for ferrite to austenite transformation; therefore, volume fraction of austenite increases with increase in weld current.

Figure 5(a)–(c) shows microstructure obtained for electrode tip diameters of 5, 6 and 7 mm, respectively, for a constant welding current of 6 kA. Volume fraction of austenite shows decreasing trend for electrode tip diameter because with increase in electrode tip diameter, contact area increases, which results in less heat generation for the same welding current and faster cooling of FZ. Therefore, the volume fraction of austenite in FZ decreases with increase in electrode tip diameter.

Microhardness profile for resistance spot welded DSS is shown in Figure 5(d). It is observed that FZ possesses higher hardness compared to BM because the individual ferrite phase is slightly harder than the austenite phase [22] and the volume fraction of ferrite in FZ is much higher than austenite. The effect of electrode tip diameter on microhardness is shown in Figure 6, which shows that electrode tip diameter does not have any significant effect on microhardness of FZ.

3.2 Physical and mechanical aspects

Figures 7 and 8 show the effect of electrode tip diameter and welding current on TSS and nugget diameter of spot welded joint of DSS. It is observed that nugget diameter and TSS increase with increase in welding current irrespective of electrode tip diameter. With increase in welding current, heat generation increases, which results in increase of nugget diameter and TSS. Similar type of effect on nugget diameter and TSS is also noted by Arabi et al. [5] and Pouranvari et al. [2] for their respective materials with the considered values of electrode tip diameter. For constant welding current, with an increase in electrode tip diameter, TSS of welded joint decreases. This is because, with increase in electrode tip diameter total heat available is divided into more area and total heat available per unit area is decreased, i.e. current density reduces, which results in reduction of TSS.

For 5 mm electrode tip diameter, when the welding current reaches 6 kA, nugget diameter reaches to its maximum value, i.e. 4.8 mm. After this, with increase in current due to high heat generation, expulsion takes place, which reduces nugget diameter and TSS of welded joint. Similarly, for 6 mm electrode tip diameter, the maximum nugget diameter is 5.6 mm and after this it

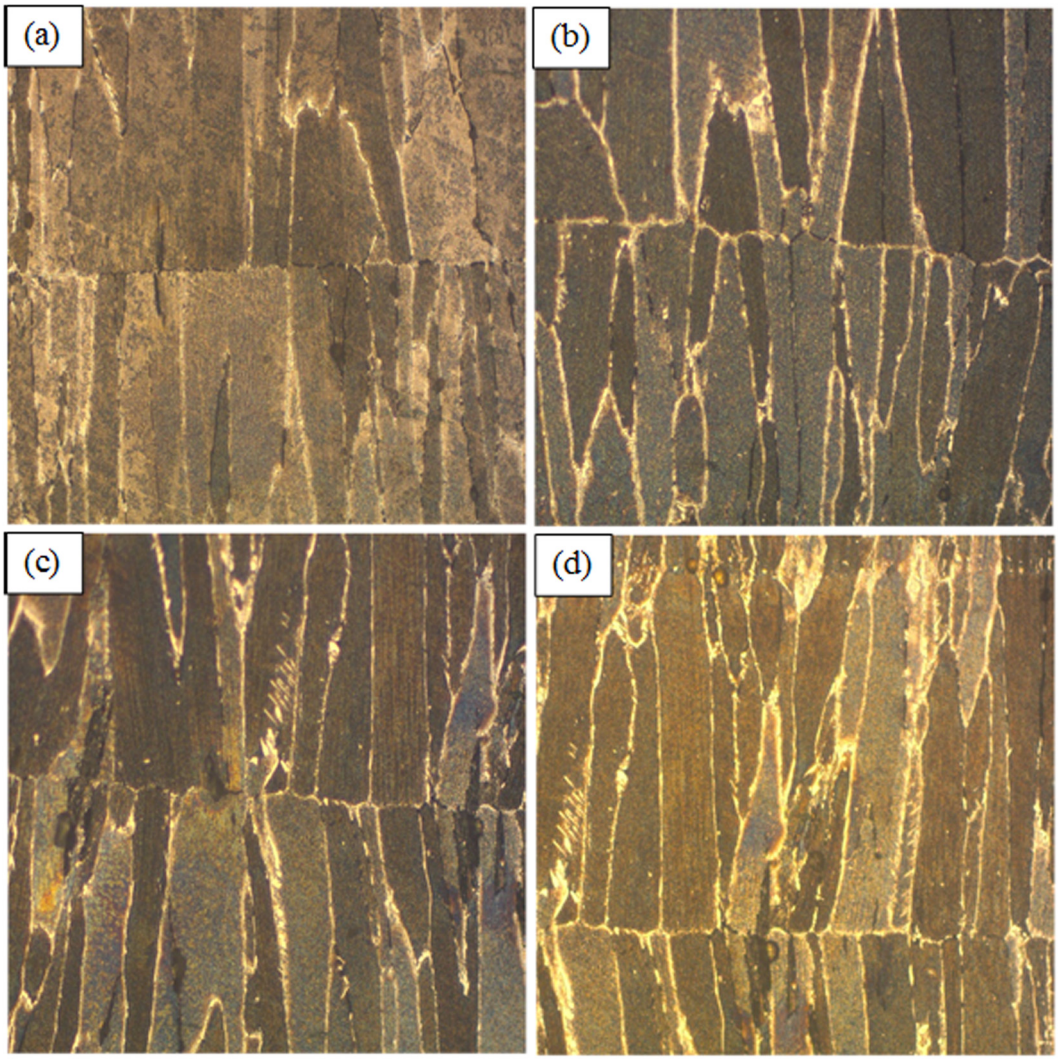

Figure 4: Effect of welding current on microstructure with 6 mm electrode tip diameter: (a) 4 kA, (b) 5 kA, (c) 6 kA and (d) 7 kA.

starts decreasing, and for 7 mm electrode tip diameter, the maximum nugget diameter is 6.318 mm. Therefore, it is concluded that maximum nugget diameter and TSS obtained for a particular electrode tip diameter are limited by expulsion phenomena. However, welding current limit observed for this expulsion can be increased by increase in electrode tip diameter.

With the help of 7 mm electrode tip diameter, it is possible to increase the nugget diameter up to 6.318 mm, but a nugget diameter higher than 5.6 mm does not have significant effect on TSS. Furthermore, it is noticed that TSS decreases with increase in electrode tip diameter for the same welding current, but maximum TSS is obtained for particular electrode tip diameter increases with increase in electrode tip diameter up to a specific value and then it remains constant. This signifies that, during the PF mode, material fails via tensile stress at the nugget circumference rather shear stress at the sheet/sheet interface.

Figure 9 shows the effect of electrode tip diameter on indentation, which shows decreasing trend of indentation with increase in electrode tip diameter. For small electrode tip diameter, due to more current intensity, electrode indentation is higher which reduces surface quality and lowers the TSS.

3.3 Failure mode

After performing the tensile shear test, failure mode of each sample is determined based on visual observation of weld fracture surfaces. A total of five different types of failure modes are observed for all experiments run, namely, IF mode, PF mode, double PF mode, partial

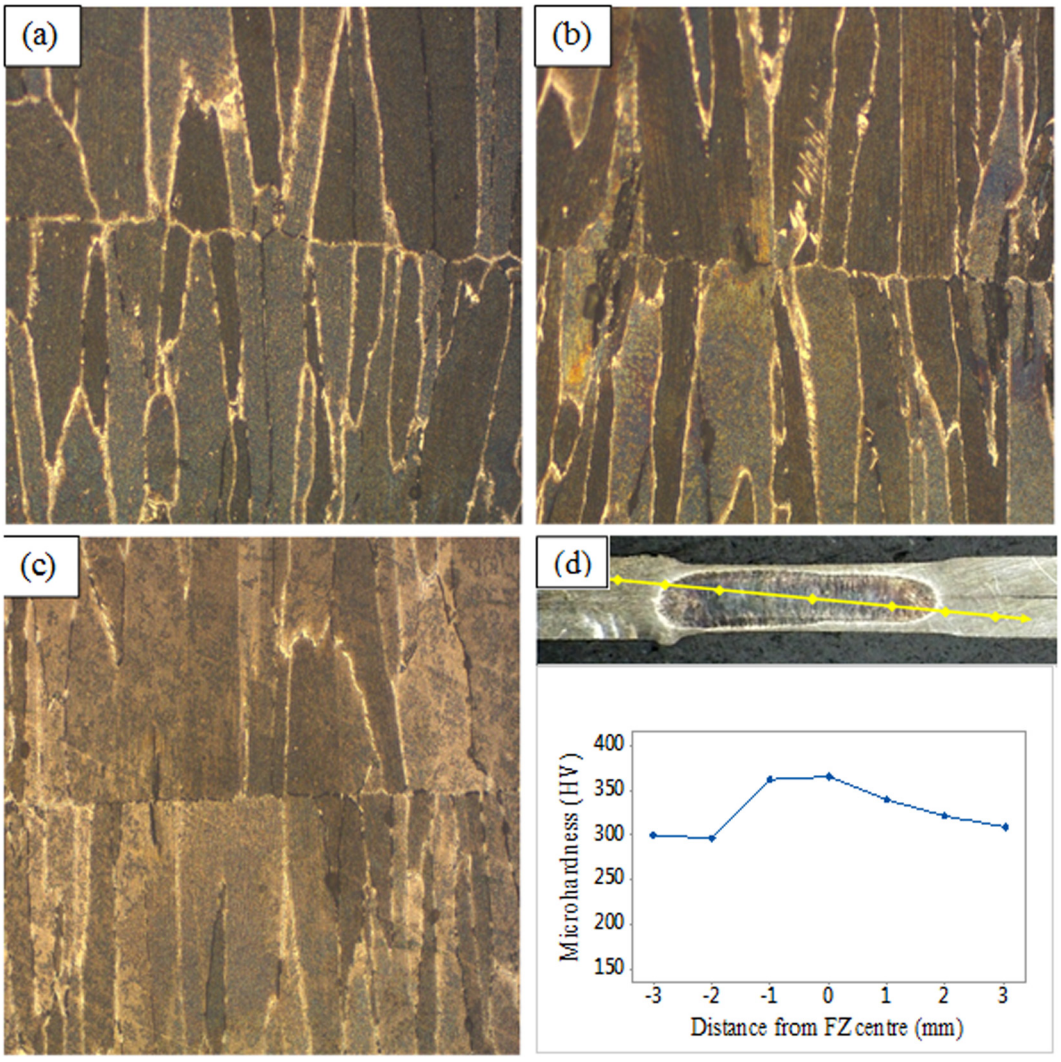

Figure 5: Effect of electrode tip diameter on microstructure with 6 kA welding current: (a) 5 mm, (b) 6 mm, (c) 7 mm and (d) microhardness profile for 2205 DSS spot welded joint.

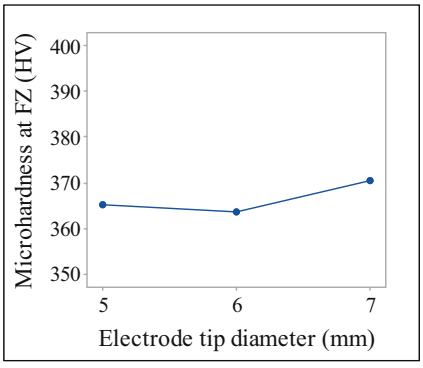

Figure 6: Effect of electrode tip diameter on microhardness of FZ.

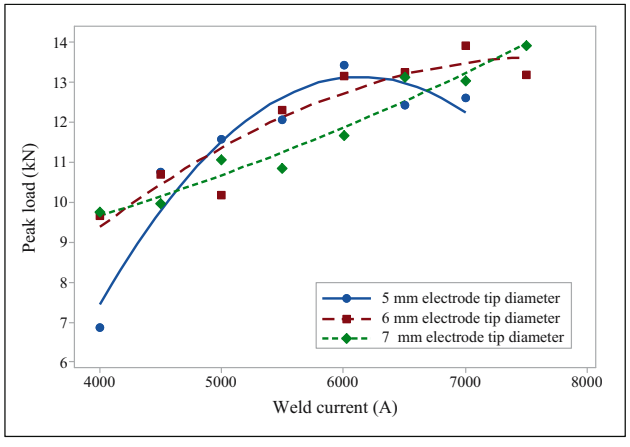

Figure 7: Effect of electrode tip diameter and welding current on peak load of tensile shear test.

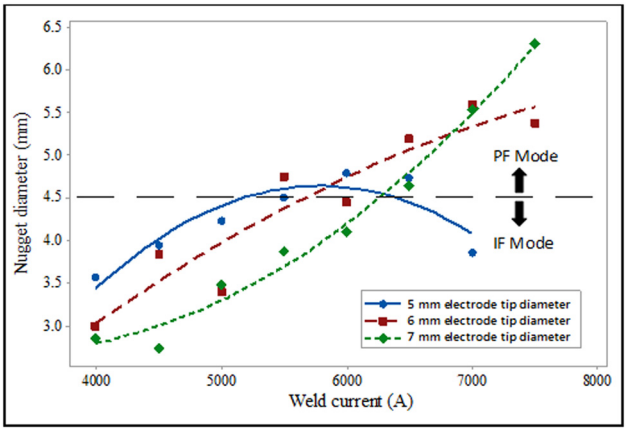

Figure 8: Effect of electrode tip diameter and welding current on nugget diameter and failure mode.

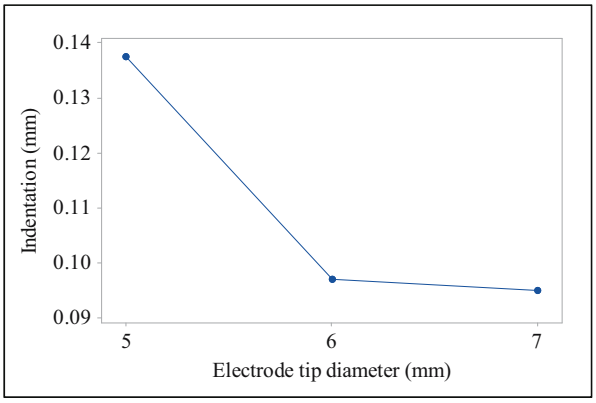

Figure 9: Effect of electrode tip diameter on electrode indentation.

thickness with PF mode and interfacial fracture with PF mode, which are shown in Figure 10. From Figure 8, it is observed that with an increase in welding current, nugget diameter increases, which results in failure mode transition from the IF mode to the PF mode. For 5 mm electrode tip diameter, when the welding current is in the range of 4–5 kA, spot welds failed through the IF mode and for the current range of 5.5–7 kA, spot welds failed through the PF mode. Similarly, for 6 and 7 mm electrode tip diameter, the PF mode is observed for 6–7.5 and 6.5–7.5 kA, respectively. It is well known documented that there is critical nugget diameter beyond which transition of the IF mode to the PF mode takes place [7]. Critical nugget diameter to ensure the PF mode is around 4.5 mm and above this diameter all samples fail in the PF mode irrespective of electrode tip diameter.

Previous research studies investigated the failure mechanism for spot welded joint and concluded that the shear stress at the sheet/sheet interface is responsible for the IF mode, whereas tensile stress at the nugget circumference is responsible for the PF mode. Furthermore, the critical nugget diameter of 3.57 mm, recommended by AWS (obtained from $4\sqrt{t}$, where t is the sheet thickness), does not ensure the PF mode for 0.8 mm 2205 DSS, whereas $5\sqrt{t}$ can provide weld with the PF mode.

4 Conclusions

A detailed experimental investigation is carried out to investigate the effect of electrode tip diameter on metallurgical and mechanical aspects of spot welded joint of 0.8 mm 2205 DSS. Based on the obtained results, the following conclusions are drawn:

- With increase in welding current, volume fraction of austenite increases. This is because, with increase in welding current, heat generation in FZ increases, i.e. temperature of FZ that increases the total available time for ferrite to austenite transformation; therefore, volume fraction of austenite increases with increase in weld current.
- With increase in electrode tip diameter, contact area increases, which results in less heat generation for the same welding current and faster cooling of FZ. Therefore, volume fraction of austenite in FZ decreases with increase in electrode tip diameter.
- Smaller electrode tip diameter limits the increase in welding current and so the increase in nugget diameter and TSS. However, maximum welding current without expulsion increases with increase in electrode tip diameter.
- TSS decreases with increase in electrode tip diameter for the same welding current, but maximum TSS obtained for particular electrode tip diameter increases with increase in electrode tip diameter up to specific limit and then it remains constant.
- Electrode indentation decreases with increase in electrode tip diameter. Due to more current intensity, electrode indentation is higher in the case of smaller electrode tip diameter, which reduces surface quality and lowers the TSS.
- Critical nugget diameter for the PF mode is around 4.5 mm for 0.8 mm 2205 DSS, which confirms that a critical nugget diameter of 3.57 mm as recommended by AWS does not ensure the PF mode for 0.8 mm 2205 DSS, whereas $5\sqrt{t}$ can provide weld with the PF mode.

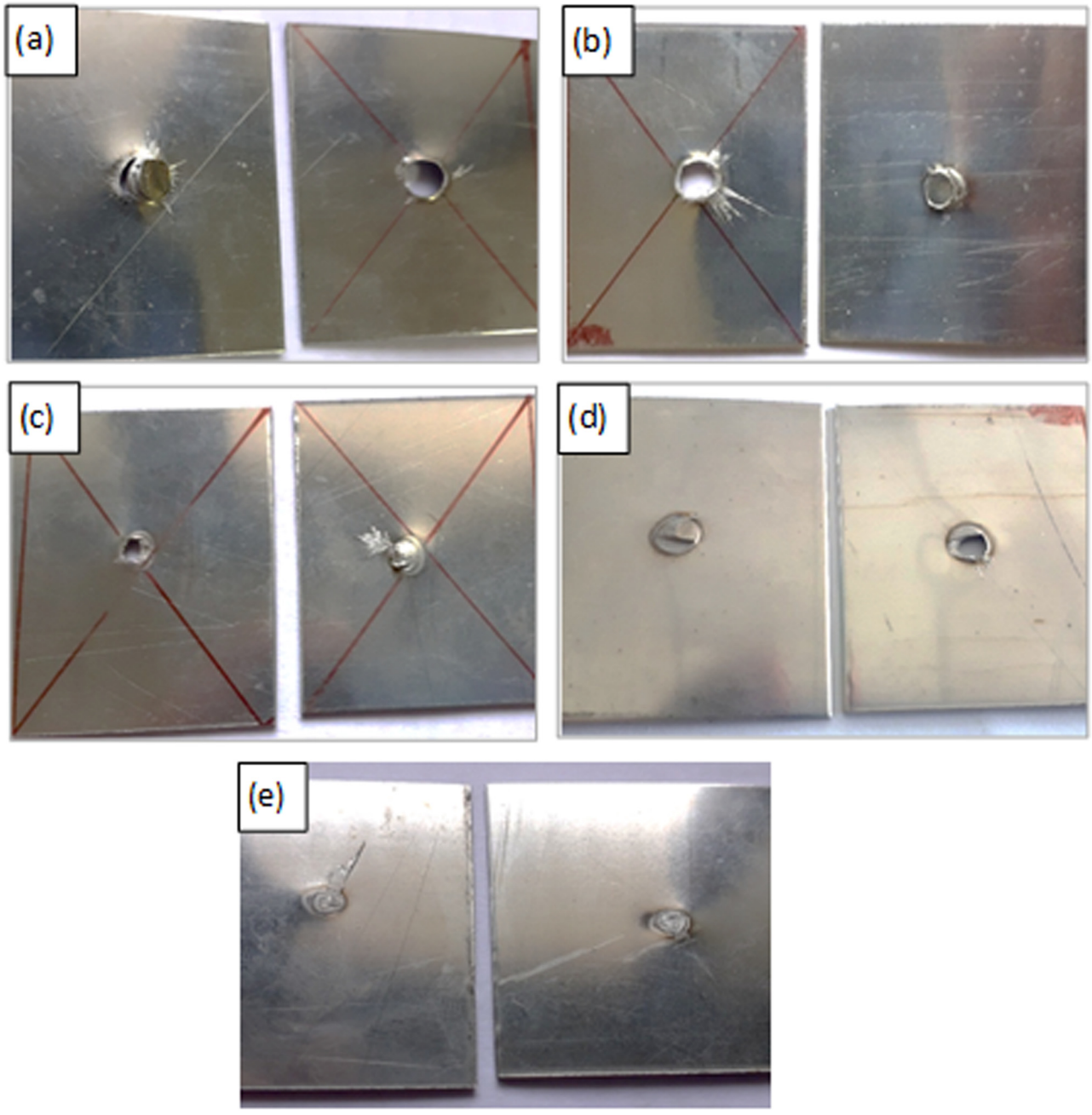

Figure 10: Various failure modes observed: (a) double PF mode, (b) PF mode, (c) partial thickness with PF, (d) interfacial fracture with PF and (e) IF mode.

Overall, TSS obtained from 6 to 7 mm electrode tip diameter is comparatively similar and higher than 5 mm electrode tip diameter, but welding current requirement for 7 mm electrode tip diameter is higher than 6 mm. Hence, by considering energy consumption, 6 mm electrode tip diameter with 7 kA welding current provides optimum TSS.

References

[1] Zuidema, B. K. Bridging the design–manufacturing–materials data gap: Material properties for optimum design and manufacturing performance in light vehicle steel-intensive body structures. *The Journal of Operations Management*, Vol. 64, 2012, pp. 1039–1047.

[2] Pouranvari, M., M. Alizadeh-Sh, and S. P. H. Marashi. Welding metallurgy of stainless steels during resistance spot welding Part

I: fusion zone. *Science and Technology of Welding and Joining*, Vol. 20, 2015, pp. 502–511.
[3] Schuberth, S., E. Schedin, T. Frohlich, and E. Ratte. Next generation vehicle – engineering guidelines for stainless steel in automotive application. *Proceedings of the 6th Stainless Steel Science and Market Conference, June 10–13, 2008*, Helsinki, Finland, 2008, pp. 637–644.
[4] Schedin, E., M. Jansson, H. L. Groth, P. O. Santacreu, and E. Ratte. Design of a stainless b-pillar – a concept evaluation using finite element simulation. *Proceedings of the International Deep Drawing Research Group (IDDRG) 2008 International Conference, June 16–18, 2008*, Olofstrom, Sweden, 2008, pp. 16–18.
[5] Arabi, M., M. Pouranvari and M. Movahedi. Welding metallurgy of duplex stainless steel during resistance spot welding. *Welding Journal*, Vol. 96, 2017, pp. 307S–318S.
[6] Pouranvari, M., and S. P. H. Marashi. Failure mode transition in AHSS resistance spot welds. Part I. Controlling factors. *Materials Science and Engineering A*, Vol. 528, 2011, pp. 8337–8343.
[7] Pouranvari, M., and S. P. H. Marashi. Critical review of automotive steels spot welding: process, structure and properties. *Science and Technology of Welding and Joining*, Vol. 18, 2013, pp. 361–403.
[8] Williams, N. T., and J. D. Parker. Review of resistance spot welding of steel sheets Part 1 Modelling and control of weld nugget formation. *International Materials Reviews*, Vol. 49, 2004, pp. 45–75.
[9] Ahedo, V., O. Martin, J. I. Santos, P. Tiedra, and J. M. Galan. Independence of EPR and PAP tests performed on resistance spot welding joints. *Corrosion Engineering, Science and Technology*, Vol. 52, 2017, pp. 418–424.
[10] Fan, Q., G. Xu, and T. Wang. The influence of electrode tip radius on dynamic resistance in spot welding. *The International Journal of Advanced Manufacturing Technology*, Vol. 95, 2018, pp. 3899–3904.
[11] Jagadeesha, T. Experimental studies in weld nugget strength of resistance spot-welded 316L austenitic stainless steel sheet. *The International Journal of Advanced Manufacturing Technology*, Vol. 93, 2017, pp. 505–513.
[12] Subrammanian, A., D. B. Jabaraj, and V. K. Bupesh Raja. Mechanical properties and microstructure of resistance spot welded joints of AISI 409M ferritic stainless steel. *Transactions of The Indian Institute of Metals*, Vol. 69, 2016, pp. 767–774.
[13] Alizadeh-Sh, M., S. P. H. Marashi, and M. Pouranvari. Resistance spot welding of AISI 430 ferritic stainless steel: Phase transformations and mechanical properties. *Materials and Design*, Vol. 56, 2014, pp. 258–263.
[14] Pouranvari, M. Fracture toughness of martensitic stainless steel resistance spot welds. *Materials Science and Engineering A*, Vol. 680, 2017, pp. 97–107.
[15] Tamizi, M., M. Pouranvari, and M. Movahedi. Welding metallurgy of martensitic advanced high strength steels during resistance spot welding. *Science and Technology of Welding and Joining*, Vol. 22, 2017, pp. 327–335.
[16] Alizadeh-Sh, M., S. P. H. Marashi, and M. Pouranvari. Microstructure–properties relationships in martensitic stainless steel resistance spot welds. *Science and Technology of Welding and Joining*, Vol. 19, 2014, pp. 595–602.
[17] Lo, K. H., C. H. Shek, and J. K. L. Lai. Recent developments in stainless steels. *Materials Science & Engineering R*, Vol. 65, 2009, pp. 39–104.
[18] Gunn, R. N. *Duplex Stainless Steels: Microstructure, Properties and Applications*. Cambridge, England: Woodhead Publishing, 1997.
[19] Alvarez-Armas, I. Duplex stainless steels: brief history and some recent alloys. *Recent Patents on Mechanical Engineering*, Vol. 1, 2008, pp. 51–57.
[20] Charles, J. Composition and properties of duplex stainless steels. *Welding in the World*, Vol. 36, 1995, pp. 43–54.
[21] Alizadeh-Sh, M., M. Pouranvari, and S. P. H. Marashi. Welding metallurgy of stainless steels during resistance spot welding Part II – heat affected zone and mechanical performance. *Science and Technology of Welding and Joining*, Vol. 20, 2015, pp. 512–521.
[22] Arabi, S. H., M. Pouranvari, and M. Movahedi. Pathways to improve the austenite–ferrite phase balance during resistance spot welding of duplex stainless steels. *Science and Technology of Welding and Joining*, Vol. 24, 2019, pp. 8–15.
[23] Li, Y., X. Cui, Z. Luo, and S. Ao. Microstructure and tensile-shear properties of resistance spot welded 22mnmob hot-stamping annealed steel. *The Journal of Materials Engineering and Performance*, Vol. 26, 2017, pp. 424–430.
[24] Long, H., Y. Hu, X. Jin, J. Shao, and H. Zhu. Effect of holding time on microstructure and mechanical properties of resistance spot welds between low carbon steel and advanced high strength steel. *Computational Materials Science*, Vol. 117, 2016, pp. 556–563.
[25] Saha, D. C., C. W. Ji, and Y. D. Park. Coating behaviour and nugget formation during resistance welding of hot forming steels. *Science and Technology of Welding and Joining*, Vol. 20, 2015, pp. 708–720.
[26] Wang, X. P., Y. Q. Zhang, J. B. Ju, J. Q. Zhang, and J. W. Yang. Characteristics of welding crack defects and failure mode in resistance spot welding of DP780 steel. *Journal of Iron and Steel Research International*, Vol. 23, 2016, pp. 1104–1110.
[27] Sajjadi-Nikoo, S., M. Pouranvari, A. Abedi, and A. A. Ghaderi. In situ post weld heat treatment of transformation induced plasticity steel resistance spot welds. *Science and Technology of Welding and Joining*, Vol. 23, 2018, pp. 71–78.
[28] Kong, J. P., and C. Y. Kang. Effect of alloying elements on expulsion in electric resistance spot welding of advanced high strength steels. *Science and Technology of Welding and Joining*, Vol. 21, 2016, pp. 32–42.
[29] Chabok, A., E. van der Aa, I. Basu, J. De Hosson, and Y. Pei. Effect of pulse scheme on the microstructural evolution, residual stress state and mechanical performance of resistance spot welded DP1000-GI steel. *Science and Technology of Welding and Joining*, Vol. 23, 2018, pp. 649–658.
[30] Mikno, Z., and Z. Bartnik. Heating of electrodes during spot resistance welding in FEM calculations. *Archives*

of Civil and Mechanical Engineering, Vol. 16, 2016, pp. 86–100.

[31] Bayramoglu M., U. Esme, and N. Geren. Effects of welding parameters on the quality of resistance spot welded SAE 1010 steel sheet. *International Journal of Materials and Product Technology*, Vol. 19, 2003, pp. 362–373.

[32] Jaber, H. L., M. Pouranvari, R. K. Salim, F. A. Hashim, and S. P. H. Marashi. Peak load and energy absorption of DP600 advanced steel resistance spot welds. *Ironmaking & Steelmaking*, Vol. 44, 2017, pp. 699–706.

[33] AWS D8.9M. *Recommended practices for test methods for evaluating the resistance spot welding behavior of automotive sheet steel materials*. Miami, Florida: American Welding Society, 2012.

[34] Lippold, J. C., and D. J. Kotecki. *Welding Metallurgy and Weldability of Stainless Steels*. Hoboken, New Jersey: John Wiley & Sons, 2005.